Fluorine-19 NMR Studies of Fluorobenzeneboronic Acids. 1. Interaction Kinetics with Biologically Significant Ligands

Robert E. London* and Scott A. Gabel

Contribution from the Laboratory of Molecular Biophysics, MD 17-05, National Institute of Environmental Health Sciences, Box 12233, Research Triangle Park, North Carolina 27709

*Received August 6, 1993**

Abstract: Kinetic studies of the interaction of 4-fluorobenzeneboronic acid and the 3-chloro-4-fluoro analog with hydroxyl ions and with several biologically significant ligands have been performed using ^{19}F line width and magnetization transfer measurements. Analysis of pH-dependent line-width data for the boronic acid–boronate equilibrium indicates that at millimolar concentrations the boronate dissociation rates are dominated by intermolecular hydroxyl ion transfer. Dissociation rate constants for the fluorobenzeneboronates due to intermolecular hydroxyl ion transfer to the corresponding boronic acid were determined to be 2.9×10^6 M^{-1} s^{-1} and 1×10^7 M^{-1} s^{-1} for 4-fluorobenzeneboronate (FBA) and 3-chloro-4-fluorobenzeneboronate (CFBA), respectively, indicating a threefold greater rate for the 3-chloro derivative. This result presumably reflects a greater tendency of CFBA toward intermolecular association. Analogously, the presence of various buffers enhanced the rate of dissociation of hydroxyl ion from 4-fluorobenzeneboronate, with values of 2×10^7 M^{-1} s^{-1} and 2.5×10^8 M^{-1} s^{-1} for the effects of phosphate and imidazole, respectively. The proton-dependent dissociation pathway in the absence of buffers is apparently not significant in the region near neutral pH. A number of bidentate boron ligands studied, including a series of carbohydrates, catechols, and α-hydroxy acids, form complexes with sufficient stability to result in slow exchange kinetics on the ^{19}F time scale. At higher pH values, multiple resonances corresponding to the various boronate complexes could often be resolved. The ^{19}F shifts for these adducts are typically close to that of the boronate anion, consistent with an sp^3-hybridized boronate structure. However, data obtained for the FBA–sorbitol adduct at lower pH values support the presence of a trigonal boronic acid–sorbitol adduct. Dissociation of several ligand–FBA complexes was studied using magnetization transfer techniques. As in the case of hydroxyl ion dissociation, the presence of buffers significantly accelerated the dissociation rate of boronate–ligand complexes. Results were generally in close agreement with previous stopped-flow kinetic measurements, although the dissociation rate constant from the catechols is about an order of magnitude faster than the rate extrapolated from lower pH stopped-flow measurements.

Introduction

Kinetic processes involving boric and boronic acids have been studied in a number of chemical[1-7] and biochemical[8,9] systems using stopped-flow and temperature-jump methods. While providing much useful data, such an approach becomes increasingly limited in complex systems containing various ligands, buffers, and other potentially interacting species. Surprisingly, although NMR has been used extensively to study boric and boronic acid equilibria in recent years,[10,11] NMR methods have generally not been used to obtain kinetic data. However, such an approach can provide considerable mechanistic insight into reversible equilibria involving hydroxylation or the formation of borate or boronate esters.

Another interesting possibility is the use of kinetic data to obtain insight into the nature of the interaction of boronic acid inhibitors with target enzymes such as serine proteases.[9,11] Studies involving boronate inhibitors have often invoked kinetic arguments as evidence for particular modes of interaction with these enzymes. Interest in this area of investigation has recently increased as a consequence of the demonstration by both ^{15}N NMR[12] and X-ray crystallography[13] of different modes of interaction involving the formation of covalent bonds between boron and the active-site serine oxygen and/or the active-site histidine nitrogen. As a consequence of the increased interest in the mechanism of action of boronic acid inhibitors, we have carried out a series of investigations on 4-fluoro-substituted benzeneboronic acids. The favorable characteristics of fluorine-19 as an NMR probe are

* Abstract published in *Advance ACS Abstracts,* March 1, 1994.

(1) Kustin, K.; Pizer, R. *J. Am. Chem. Soc.* **1969**, *91*, 317-322.
(2) Friedman, S.; Pace, B.; Pizer, R. *J. Am. Chem. Soc.* **1974**, *96*, 5381-5384.
(3) Kajimoto, O.; Saeki, T.; Nagaoka, Y.; Fueno, T. *J. Phys. Chem.* **1977**, *81*, 1712-1716.
(4) Pizer, R.; Babcock, L. *Inorg. Chem.* **1977**, *16*, 1677-1681.
(5) Babcock, L.; Pizer, R. *Inorg. Chem.* **1980**, *19*, 57-61.
(6) Babcock, L.; Pizer, R. *Inorg. Chem.* **1983**, *22*, 174-176.
(7) Pizer, R.; Selzer, R. *Inorg. Chem.* **1984**, *23*, 3023-3026.
(8) (a) Johnson, S. L.; Smith, K. W. *Biochemistry* **1976**, *15*, 553-559. (b) Johnson, S. L.; Smith, K. W. *Biochemistry* **1976**, *15*, 560-565. (c) Johnson, S. L.; Smith, K. W. *J. Org. Chem.* **1977**, *42*, 2580-2589.
(9) (a) Nakatani, H.; Uehara, Y.; Hiromi, K. *J. Biochem. (Tokyo)* **1975**, *78*, 611-616. (b) Nakatani, H.; Hiromi, K. *Biochim. Biophys. Acta* **1978**, *524*, 413-417. (c) Nakatani, H.; Morita, T.; Hiromi, K. *Biochim. Biophys. Acta* **1978**, *525*, 423-428.
(10) (a) Yoshino, K.; Oguchi, S.; Shimakata, Y.; Mori, Y.; Okamoto, M.; Kotaka, M.; Kakihana, H. *Kyoto Daigaku Genshiro Jikkensho, [Tech. Rep.]* **1985**, KURRI-TR-260, 221-232. (b) Makkee, M.; Kieboom, A. P. G.; van Bekkum, H. *Recl. Trav. Chim. Pays-Bas* **1985**, *104*, 230-235. (c) Bell, C. F.; Beauchamp, R. D.; Short, E. L. *Carbohydr. Res.* **1986**, *147*, 191-203. (d) Bell, C. F.; Gallagher, B. C.; Lott, K. A. K.; Short, E. L.; Walton, L. *Polyhedron* **1991**, *10*, 613-618. (e) Sinton, S. W. *Macromolecules* **1987**, *20*, 2430-2441. (f) van Duin, M.; Peters, J. A.; Kieboom, A. P. G.; van Bekkum, H. *J. Chem. Soc., Perkin Trans. 2* **1987**, 473-478. (g) Chapelle, S.; Verchere, J.-F. *Tetrahedron* **1988**, *44*, 4469-4482. (h) Chapelle, S.; Verchere, J.-F. *Carbohydr. Res.* **1989**, *191*, 63-70. (i) Coddington, J. M.; Taylor, M. J. *J. Coord. Chem.* **1989**, *20*, 27-38. (j) van Haveren, J.; Peters, J. A.; Batelaan, J. G.; Kieboom, A. P. G.; van Bekkum, H. *Recl. Trav. Chim. Pays-Bas* **1989**, *108*, 179-184. (k) van Haveren, J.; van den Burg, M. H. B.; Peters, J. A.; Batelaan, J. G.; Kieboom, A. P. G.; van Bekkum, H. *J. Chem. Soc., Perkin Trans. 2* **1991**, 321-327.
(11) (a) Adebodun, F.; Jordan, F. *J. Am. Chem. Soc.* **1988**, *110*, 309-310. (b) Adebodun, F.; Jordan, F. *J. Cell Biochem.* **1989**, *40*, 249-260. (c) Baldwin, J. E.; Claridge, T. D. W.; Derome, A. E.; Schofield, C. J.; Smith, B. D. *Bioorg. Med. Chem. Lett.* **1991**, *1*, 9-12. (d) Baldwin, J. E.; Claridge, T. D. W.; Derome, A. E.; Smith, B. D.; Twyman, M.; Waley, S. G. *J. Chem. Soc., Chem. Commun.* **1991**, 573-574. (e) Zhong, S.; Jordan, F.; Kettner, C.; Polgar, L. *J. Am. Chem. Soc.* **1991**, *113*, 9429-9435.
(12) Bachovchin, W. W.; Wong, W. Y. L.; Farr-Jones, S.; Shenvi, A. B.; Kettner, C. A. *Biochemistry* **1988**, *27*, 7689-7697. (b) Farr-Jones, S.; Smith, S. O.; Kettner, C. A.; Griffin, R. G.; Bachovchin, W. W. *Proc. Natl. Acad. Sci. U.S.A.* **1989**, *86*, 6922-6924.
(13) (a) Bone, R.; Frank, D.; Kettner, C. A.; Agard, D. A. *Biochemistry* **1989**, *28*, 7600-7609. (b) Takahashi, L. H.; Radhakrishnan, R.; Rosenfield, R. E. R.; Meyer, E. F., Jr. *Biochemistry* **1989**, *28*, 7610-7617.

well-known, and it was anticipated that, analogous to the case of 4-fluoroanilines,[14] the fluorine substituent would provide a sensitive probe of hybridization changes involving the boron.

Materials and Methods

The 4-fluorobenzeneboronic acid (FBA)[15] and 3-chloro-4-fluorobenzeneboronic acid (CFBA) were obtained from Lancaster Synthesis, and all other chemicals were obtained from Sigma Chemical Co. or Aldrich Chemical Co. Fluorine-19 NMR studies were carried out on a Nicolet NT-360 multinuclear NMR spectrometer using a 5-mm ^{1}H probe retuned to the fluorine frequency of 339.7 MHz or on a GE GN-500 multinuclear spectrometer using a 5-mm fluorine probe tuned to 470.52 MHz, as indicated. ^{19}F chemical shifts were determined relative to internal trifluoroacetic acid (TFA). Spectral resolution was 0.1 ppm, but the primary contribution to errors in shift determination arises from uncertainty in the pH and is therefore a function of $|pH - pK|$ for the compound under study. For measurements of the resonance line width, proton decoupling was not used in order to avoid any local heating effects which could perturb the kinetics. However, concentrations of the boronic acids and other sample constituents were generally selected so that the exchange contribution to the line width greatly exceeded the contributions of field inhomogeneity and unresolved proton coupling. Exchange contributions were determined using 4-fluoroaniline in a capillary as a line-width standard. Although the field homogeneity in the capillary might be expected to differ somewhat from that of the sample, the line width of the standard was in very close agreement with the line widths of the fluorinated boronic acids at extreme pH values, at which the exchange contributions become negligible, suggesting that the primary contributions in both systems arise from unresolved proton couplings.

Boronic acid–ligand kinetics were determined using magnetization transfer methods. Since spectra typically contained only two resonances corresponding to boronic acid and boronate ester, magnetization transfer studies were carried out using the selective inversion technique of Robinson et al.,[16] which has the advantage that frequency-selective pulses are not required. The analysis of the data was based on the approach described by Perrin and Engler[17] in which two series of experiments are carried out with the resonance of the uncomplexed species or the adduct selectively inverted. The data are then organized into a series of 2 × 2 matrices, $\mathbf{M}(t_m)$, corresponding to each time point, the matrix corresponding to the fully relaxed system is subtracted, and the data are analyzed by matrix methods according to the relation

$$\ln(\mathbf{M}\mathbf{M}_0^{-1}) = \mathbf{X}(\ln \Lambda)\mathbf{X}^{-1} = -t_m\mathbf{R} \qquad (1)$$

where $\mathbf{M}_0$ corresponds to the data matrix at $t_m = 0$ and $\mathbf{X}$ is a square matrix of eigenvectors that transforms $\mathbf{M}\mathbf{M}_0^{-1}$ into the diagonal matrix Λ. A linear fit of the data then yields the relaxation matrix $\mathbf{R}$, in which the diagonal elements correspond to $1/T_{1F} + k_{FB}$ and $1/T_{1B} + k_{BF}$ and the off-diagonal elements to k_{FB} and k_{BF}. Here k_{BF} and k_{FB} are the apparent first-order rate constants for the dissociation and association reactions, and T_{1F} and T_{1B} are the spin–lattice relaxation times for the free and bound species, respectively. In general, the optimal series of delays t_m for the determination of the rate constants can differ significantly from the optimal delays for the determination of accurate T_1 values. In this case, since the major interest was the determination of the rates, the delays were incremented regularly and arranged so that the longest delay was $\sim k_{BF}^{-1} \sim k_{FB}^{-1}$, where the latter approximate equality was satisfied by using ligand concentrations sufficient so that the resonance intensities for the free and bound species were similar. Since the diagonal elements of the relaxation matrix correspond to sums of exchange rates and spin–lattice relaxation rates, the numerical values for one or the other of these parameters can be subject to a large error if the contribution to the sum is small. For example, if $1/T_{1F} \ll k_{FB}$, in general the error in $1/T_{1F}$ can be substantial. Data were analyzed using a program written in Mathematica. Repeated measurements on the same sample and analysis using the above program yielded extremely consistent results, with rate constants within 5% of each other. Reproducibility of separate samples with nominally identical composition was <15%. One of the interesting aspects of this analytical approach is that the multiplication of one of the component resonances by a constant factor does not alter the derived rate constants. Consequently, peak heights rather than peak areas can be used for the measurements if the ratio of the line widths of the two resonances remains constant.

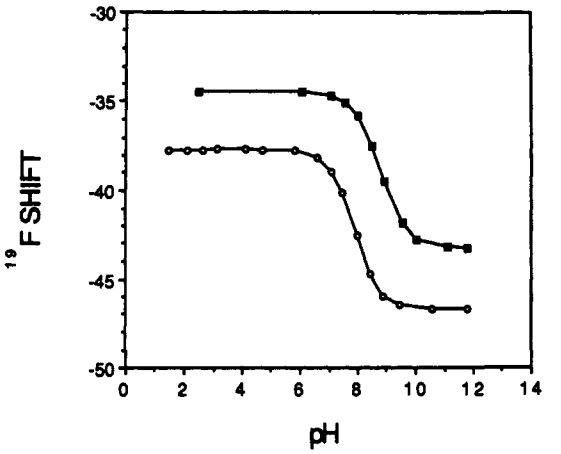

Figure 1. ^{19}F chemical shifts for FBA (□) and CFBA (○) as a function of pH.

Results

The fluorine resonances of 4-fluorobenzeneboronic acid (FBA) and 3-chloro-4-fluorobenzeneboronic (CFBA) acids undergo upfield titration shifts of 8.8 and 9.0 ppm, respectively, corresponding to the hydroxylation of the boron (Figure 1). pK values of 8.7 and 7.9 for FBA and CFBA, respectively, were obtained from these curves. These chemical shifts are similar in magnitude but opposite in direction to the shift observed upon protonation of the amino group in 4-fluoroaniline.[14] In both cases, there is a change in hybridization of the substituent para to the fluorine reporter group from sp^2 to sp^3. At a field strength of 8.5 T and a temperature of 21 °C and using 10 mM concentrations, the exchange between boronate and boronic acid species was found to be intermediate on the NMR time scale for FBA but fast for CFBA. This result was initially somewhat surprising, since the dissociation rate constant of the more strongly bound hydroxyl group of CFBA was expected to be slower than the dissociation rate of the hydroxyl from FBA. Indeed, the expected relationship was obtained by Kajimoto et al.,[3] using stopped-flow techniques, who find dissociation rate constants of 413 and 156 s^{-1} for benzeneboronic and 3-chlorobenzeneboronic acids, respectively, at 35 °C, 0.1 M KCl. Due to the small Hammett constant of the para fluorine substituent, these values would be expected to approximate those of the corresponding fluorinated benzeneboronic acids. The dissociation rates obtained by Kajimoto et al.[3] are sufficiently slow to lead to slow exchange at the fields studied ($\tau\Delta\nu \gg 1$), so that the observed spectra indicate that, under the conditions of the present study, significant catalysis of the hydroxyl exchange reaction is occurring.

Insight into the basis for the faster hydroxyl ion exchange rates obtained from the NMR studies was obtained by noting that the exchange-broadened resonances narrowed considerably in the presence of various buffer systems, including phosphate, Tris, and Tris-HEPES. The effect of 0.05 M phosphate buffer on the exchange rate is illustrated in Figure 2. In addition to acting as an exchange catalyst, Tris was also found to form specific complexes with borate, similar to those observed for other polyols. The most likely mechanism for such an effect would involve acid catalysis, with a proton transferred from the buffer to the boronate species and subsequent loss of water to form the boronic acid. Thus, the phosphate group facilitates loss of a hydroxyl ligand by proton transfer and, conversely, the binding of hydroxyl groups by accepting a proton from an incoming water molecule (Figure 3). These results suggest that the hydroxylation kinetics observed in the absence of buffer may reflect intermolecular interactions,

(14) (a) Smith, G. A.; Hesketh, R. T.; Metcalfe, J. C.; Feeney, J.; Morris, P. G. *Proc. Natl. Acad. Sci. U.S.A.* **1983**, *80*, 7178–7182. (b) Levy, L. A.; Murphy, E.; Raju, B.; London, R. E. *Biochemistry* **1988**, *27*, 4041–4048. (c) Deutsch, C. J.; Taylor, J. S. *Biophys. J.* **1989**, *55*, 799–804.

(15) Abbreviations: BBA, benzeneboronic acid; CFBA, 3-chloro-4-fluorobenzeneboronic acid; FBA, 4-fluorobenzeneboronic acid; FBOH$^-$, 4-fluorobenzeneboronate; NMR, nuclear magnetic resonance.

(16) Robinson, G.; Kuchel, P. W.; Chapman, B. E.; Doddrell, D. M.; Irving, M. G. *J. Magn. Reson.* **1985**, *63*, 314–319.

(17) Perrin, C. L.; Engler, R. E. *J. Magn. Reson.* **1990**, *90*, 363–369.

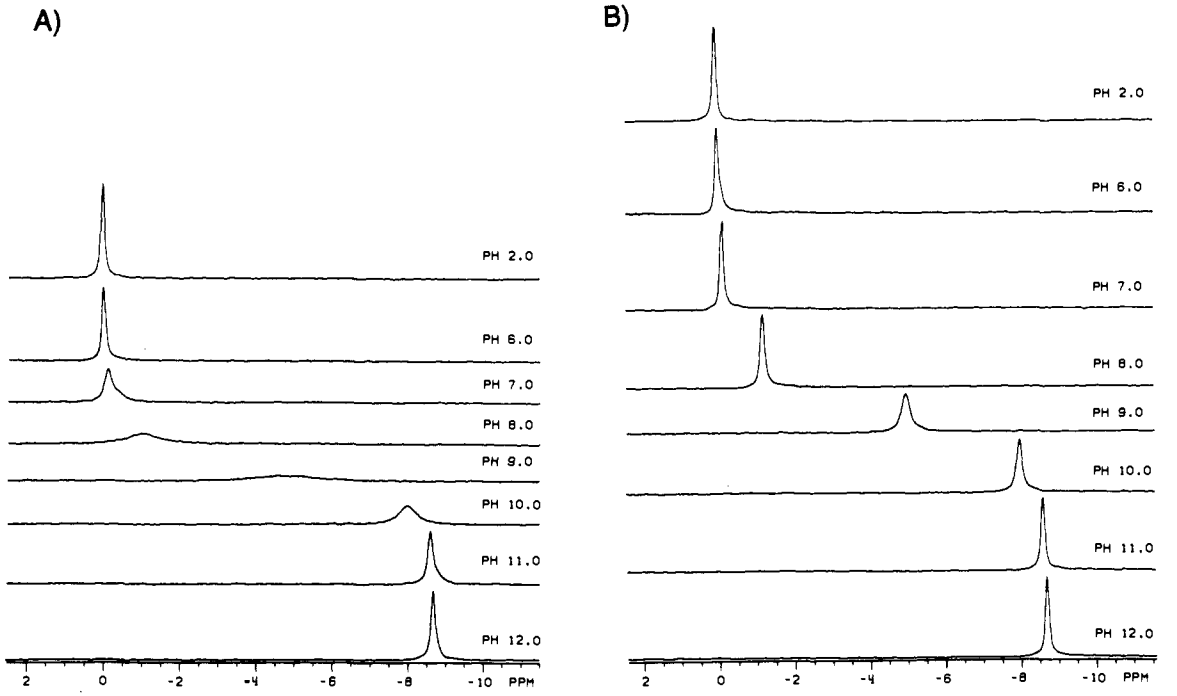

Figure 2. (A) ^{19}F NMR spectra (339.7 MHz) of 10 mM 4-fluorobenzene boronic acid (FBA) as a function of pH. The chemical shift of FBA at low pH was arbitrarily set to 0. (B) ^{19}F NMR spectra (339.7 MHz) of 10 mM FBA obtained at the pH values indicated in 50 mM phosphate buffer.

with the boronic acid itself acting in a fashion analogous to that of the buffer, although a transfer of a hydroxyl ion rather than a proton would be involved. In order to obtain a more detailed, quantitative understanding of these phenomena, a series of line-width measurements was carried out and analyzed as described below.

Dissociation Rate Constant Analysis

In order to quantitatively analyze the effects of various interactions on the hydroxylation/dehydroxylation kinetics of FBA, a strategy was developed involving a comparison of experimental dissociation rate constants derived from line-width data using the well-known Luz and Meiboom relationship[18] with theoretical determinations based on various model interactions. Concentrations of FBA and/or other constituents of the sample were adjusted so that the exchange rate would fall into the fast exchange limit, allowing use of the simple expression for $1/T_2$ in terms of the bound (boronate) and free (boronic acid) species:

$$\frac{1}{T_2} = \frac{p_F}{T_{2F}} + \frac{p_B}{T_{2B}} + p_F{}^2 p_B{}^2 \Delta\omega^2(\tau_F + \tau_B) \qquad (2)$$

$$= \frac{1-p_B}{T_{2F}} + \frac{p_B}{T_{2B}} + p_B(1-p_B)^2\Delta\omega^2\tau_B \qquad (3)$$

where p_F (p_B), τ_F (τ_B), and T_{2F} (T_{2B}) correspond to the fractional concentration, the lifetime, and the transverse relaxation times of the boronic acid (boronate) species and $\Delta\omega$ is the chemical shift difference. Equations 2 and 3 are valid in the fast exchange limit at which the lifetime of the bound state falls below the transition point, $\tau_B \ll \sqrt{2}/(\pi\Delta\nu)$. Numerical calculations indicate than, in order to obtain a reasonably Lorentzian line shape, the bound lifetime must be at least fivefold shorter than this transition value. Setting $T_{2F} = T_{2B} = T_2°$, since the transverse relaxation times for both species are similar and relatively long, and setting the experimental dissociation rate constant $k_{off} = 1/\tau_B$ in equation 3 gives:

$$k_{off} = \frac{p_B(1-p_B)^2\Delta\omega^2}{1/T_2 - p_B/T_{2B} - p_F/T_{2F}} = \frac{p_B(1-p_B)^2\Delta\omega^2}{1/T_2 - 1/T_2°} \qquad (4)$$

where experimentally $1/T_2°$ was determined from the reference compound. For a simple reversible hydroxyl ion binding equilibrium described by the relation

$$\mathrm{FBA} + \mathrm{OH^-} \underset{k_{-1}}{\overset{k_1}{\rightleftharpoons}} \mathrm{FBOH^-} \qquad (5)$$

where FBA corresponds to fluorobenzeneboronic acid and $FBOH^-$ to fluorobenzeneboronate, $k_{off} = k_{-1}$ will be constant. Alternatively, the effects of buffers on the line width suggest the possibility of a pH-dependent dissociation:

$$\mathrm{FBA} + \mathrm{H_2O} \underset{k_{-2}}{\overset{k_2}{\rightleftharpoons}} \mathrm{FBOH^-} + \mathrm{H_3O^+} \qquad (6)$$

In this case, the lifetime of the $FBOH^-$ can be represented by a pseudo-first-order rate constant $k'_{-2} = k_{-2}[H^+] = k_{-2}10^{-pH}$. Finally, it is necessary to include the possibility of intermolecular hydroxyl ion transfer, described by

$$\mathrm{FBA} + \mathrm{FB^*OH^-} \underset{k_{-3}}{\overset{k_3}{\rightleftharpoons}} \mathrm{FBOH^-} + \mathrm{FB^*A} \qquad (7)$$

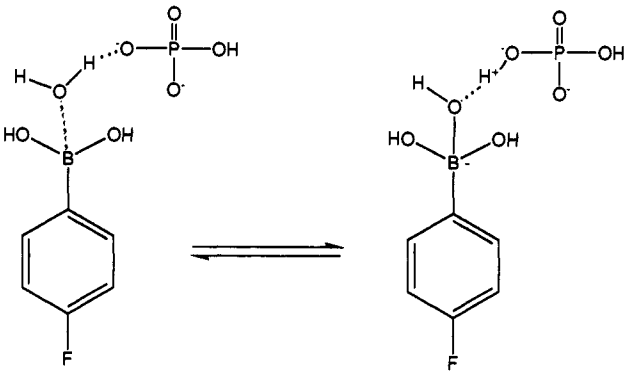

Figure 3. Proposed basis for the catalysis of boronic acid hydroxyl group exchange by inorganic phosphate.

(18) Meiboom, S.; Luz, Z.; Gill, D. *J. Chem. Phys.* **1957**, *27*, 1411–1412.

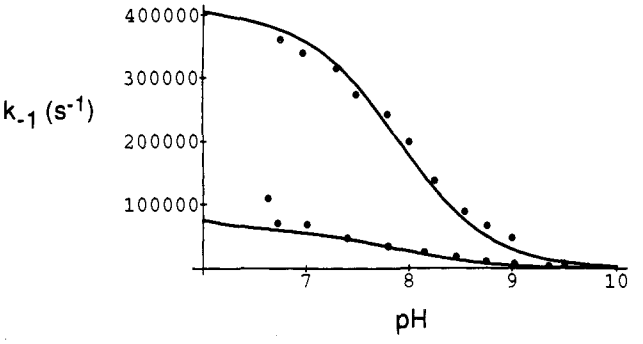

Figure 4. Hydroxyl ion dissociation rate constants k_{off} determined from line-width measurements in samples containing 6 mM CFBA (lower curve) or 50 mM CFBA (upper curve) measured as a function of pH. The theoretical curves correspond to eqs 8 and 9 with parameters given in Table 1: sample temperature = 21 °C; 0.1 M KCl.

Table 1. $FBOH^-$ Dissociation Rate Constants[a]

boronic acid	k_{-1}	$10^{-10}k_{-2}$	k_{-3}	k_{-4}
CFBA	$<10^3$	<1.6	1×10^7	
FBA	$<10^3$	<1.6	2.9×10^6	
+ Phosphate				2×10^7
+ Imidazole				2.5×10^8

[a] Units are s^{-1} (k_{-1}) or $M^{-1}\,s^{-1}$ (k_{-2}, k_{-3}, and k_{-4}). Rate constants were measured at T = 21 °C.

In this case, the dissociation of $FBOH^-$ can again be described by a pseudo-first-order dissociation rate constant given by

$$k'_{-3} = k_{-3}[FBA] = \frac{k_{-3}[BA_0]10^{(pK_B-pH)}}{1 + 10^{(pK_B-pH)}} \quad (8)$$

where $[BA_0] = [FBA] + [FBOH^-]$ is the total concentration of boronic acid plus boronate, which is held constant as the pH is varied, and pK_B is the pK of the boronic acid, determined from the titration curves to be 8.7 for FBA and 7.9 for CFBA.

The experimental line-width data are thus analyzed by setting

$$k_{off} = k_{-1} + k'_{-2} + k'_{-3} \quad (9)$$

The contributions of the three dissociation mechanisms are easily compared, since they exhibit very different pH-dependent behavior. Experimental points and a theoretical plot of k_{off} corresponding to data obtained at two CFBA concentrations are shown in Figure 4. These data show clearly that, at the concentrations of boronic acid used in these studies, the third mechanism corresponding to intermolecular hydroxide ion transfer (eq 8) is completely dominant. Fitting the data to eqs 8 and 9 gives $k_{-3} = 1 \times 10^7\ M^{-1}\,s^{-1}$. Only upper limits for k_{-1} and k_{-2} of $10^3\ s^{-1}$ and $1.6 \times 10^{10}\ M^{-1}\,s^{-1}$, respectively, can be obtained from this study. The results are summarized in Table 1. As noted in the previous section, the FBA kinetics tended to fall into the intermediate exchange limit at concentrations of several millimolar, so that higher FBA concentrations were required to carry out analogous experiments. Analogous studies using FBA (Figure 5, curve a) give $k_{-3} = 2.9 \times 10^6\ M^{-1}\,s^{-1}$, only about one third the rate obtained for CFBA. Hence, the intermolecular hydroxide ion transfer process is considerably more favorable for CFBA than for FBA. This result presumably reflects the greater tendency for the more hydrophobic CFBA molecules to associate.

Effects of buffers on the dissociation rate constant of the boronate species can be taken into account by including an additional term corresponding to the reaction

$$FBA + BUF + H_2O \underset{k_{-4}}{\overset{k_4}{\rightleftharpoons}} FBOH^- + BUF/H^+ \quad (10)$$

The corresponding pseudo-first-order dissociation rate constant

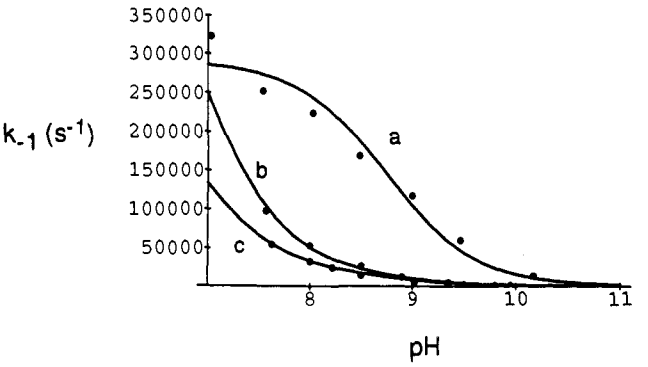

Figure 5. Hydroxyl ion dissociation rate constants k_{off} for FBA as a function of pH determined under the following conditions: (a) 100 mM FBA; (b) 6 mM FBA, 30 mM imidazole; (c) 6 mM FBA, 15 mM imidazole. The theoretical curves correspond to a sum of four contributions to the dissociation rate, with parameters given in Table 1.

is given by

$$k'_{-4} = k_{-4}[BUF/H^+] = \frac{k_{-4}[BUF_0]10^{(pK'-pH)}}{1 + 10^{(pK'-pH)}} \quad (11)$$

where $[BUF_0]$ is the total buffer concentration and pK' is the pK value for the particular buffer. Data obtained for 6 mM FBA and phosphate (pK = 6.8) buffer concentrations of 30 and 15 mM are shown in Figure 5. As can be seen from the figure, the presence of buffer shifts the rate acceleration effect from the pK of the FBA toward the lower pK of the buffer. A fit of the two curves (Figure 5b and c) obtained in the presence of phosphate gave $k_{-4} = 2 \times 10^7\ M^{-1}\,s^{-1}$. It was expected that an imidazole buffer (pK = 6.92) would result in a larger value of k_{-4} than the phosphate buffer, since the interaction of the $H_2PO_4^-$ ion with the $FBOH^-$ involves two anionic species. Data obtained in the presence of imidazole (not shown) gave $k_{-4} = 2.5 \times 10^8\ M^{-1}\,s^{-1}$, an order of magnitude greater than the corresponding rate for the phosphate interaction. In addition to its action as a dehydroxylation catalyst, the imidazole can also serve as a boron ligand.[19] However, the binding of the monodentate imidazole ligand is relatively weak, and most of the rate enhancement occurs at lower pH, corresponding to the protonated imidazolium, which does not function as a ligand. On the basis of the rate constants summarized in Table 1, it was predicted that a 1 mM solution of FBA with the pH set near the pK value of 8.7 would exhibit slow exchange kinetics at a field of 11.75 T in the absence of additional buffers. This prediction was verified experimentally.

Point of Maximum Line Width

In the analysis of reversible binding equilibria we have found that the shape of the line width or $1/T_2$ curves vs pH provides a useful indicator of dissociation mechanism. As noted elsewhere,[20] the maximum line width corresponding to a simple dissociative process as in eq 5 occurs when the fraction of ligand which is complexed, p_B, is given by

$$p_B^{MB} = {}^2/_3 - [{}^1/_9 - (1/T_{2B} - 1/T_{2F})/(3\Delta\omega^2\tau_B)]^{1/2} \quad (12)$$

For small molecules, the second term in the radical is generally negligible, and the maximum broadening occurs at $p_B \sim {}^1/_3$. Thus, the maximum line width will not coincide with the pK of the molecule but corresponds to

(19) Koehler, K. A.; Jackson, R. C.; Lienhard, G. E. *J. Org. Chem.* **1972**, *37*, 2232–2237.
(20) (a) Lenkinski, R. E.; Reuben, J. *J. Magn. Reson.* **1976**, *21*, 47–56. (b) London, R. E. *J. Magn. Reson.* **1993**, *A104*, 190–196.
(21) de Bruyn, A.; Anteunis, M. *Acta Cienc. Indica* **1976**, *2*, 1–4.

$$p_B = \frac{1}{1 + 10^{(pK_B - pH)}} = \frac{1}{3} \quad (13)$$

$$pH^{MB} = pK_B - \log(2) \quad (14)$$

Thus, the maximum line width is displaced by $\log(2) \sim 0.3$ pH units below the boronic acid pK. (An upward displacement would be observed for a more typically encountered protonation equilibrium.) In contrast, for a process dominated by an associative equilibrium as described by eq 7, $k_{off} = k_{-3}p_F[BA]$, where $p_F[BA]$ corresponds to the fraction of molecules in the boronic acid form. In this case, eq 2 becomes

$$\frac{1}{T_2} = \frac{1 - p_B}{T_{2F}} + \frac{p_B}{T_{2B}} + \frac{p_B(1 - p_B)\Delta\omega^2}{k_{-3}[BA]} \quad (15)$$

corresponding to a maximum line width at

$$p_B^{MB} = \frac{1}{2} + \frac{(1/T_{2B} - 1/T_{2F})k_{-3}[BA]}{2\Delta\omega^2} \quad (16)$$

Making the same approximation as above, $p_B^{MB} \sim {}^1/_2$, leading to $pH^{MB} = pK$. Hence, a significant displacement of the maximum line width is observed for a simple dissociation process, as described by eq 5, but not for an associative process as described by eq 7. This result is consistent with the observed dependence of line width on pH, which was not observed to be displaced significantly from the pK value of the boronic acid under study.

Interaction with Ligands

Since the ultimate goal of the present studies is an evaluation of the biological effects of boronic acids, the interactions of FBA with various biologically significant ligands were evaluated. Although there are at present substantial reports of such interactions in the literature (e.g. see refs 2, 7, 8, and 10), the majority of these studies have been carried out at nonphysiological pH and concentration ranges, and there are apparently no reports on interactions with phosphorylated glycolytic intermediates. In the cases studied involving bidentate boron ligands, the ligand exchange rates were sufficiently slow to allow observations of liganded and unliganded species. For these cases, the ^{19}F resonance of the former undergoes a significant upfield shift with magnitude similar to that observed upon conversion of 4-fluorobenzeneboronic acid to 4-fluorobenzeneboronate. Typical spectra obtained for a variety of bidentate ligands are shown in Figure 6, and the ^{19}F shifts of the complexes relative to those of trifluoroacetate or to the (uncomplexed) FBA resonance at pH 7.2 are summarized in Table 2. Thus, these shift and kinetic data are consistent with the conclusion that in all cases the complex formed involves the anionic, boronate species (however, see below). Similar conclusions for boric and benzeneboronic acid (BBA) have resulted from analysis of the ^{11}B NMR resonances.[10] Several trends are readily apparent; e.g., the shifts (relative to FBA) associated with binding to the aldoses were larger than those corresponding to binding to the polyols or the anions.

Although at neutral pH only a single fluorine resonance for each adduct was generally observed, in most cases the resonances sharpen and multiple peaks become observable as the pH is raised, analogous to results of ^{11}B NMR studies of borate complexes at high pH.[10b] The increased stability of the adducts at high pH may arise from a reduction in the intermolecular ligand transfer rates, analogous to the case of the intermolecular hydroxyl ion transfer discussed above, i.e. processes described by

$$FBA + FB^*\text{–}L \rightleftharpoons FB\text{–}L + FBA^* \quad (17)$$

where FB–L is the boronate ligand complex and FBA the boronic acid. Additionally, proton catalysis or catalysis involving protonated ligands such as lactic acid will also be reduced at high pH. Exchange processes were generally found to be sufficiently slow at high pH to readily allow resolution of chemical shift differences of <0.1 ppm. In general, observation of multiple ^{19}F resonances can arise due to three effects: (1) multiple modes of adduct formation; (2) formation of adducts with higher boronic acid/ligand stoichiometry—for example, the shifts observed in a diboronate complex may differ from those observed in the corresponding monoboronate complexes; (3) in some cases, adduct formation resulting in formation of a chiral center at the boron nucleus; for ligands containing at least one chiral center, the resulting diastereomers may exhibit distinct chemical shifts.

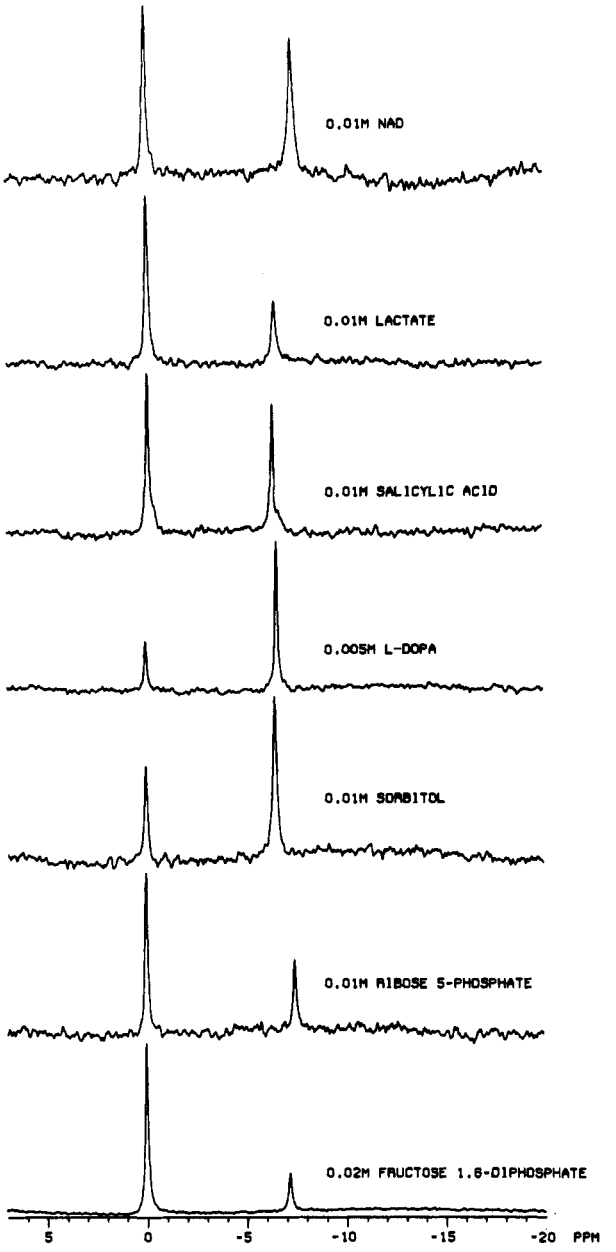

Figure 6. ^{19}F NMR spectra (339.7 MHz) of 1.5 mM FBA in the presence of NAD^+, L-lactate, salicylate, L-DOPA, sorbitol, ribose-5-phosphate, or fructose 1,6-diphosphate as indicated. The ligand concentration was 10 mM, except in the case of L-DOPA (5 mM) and fructose-1,6-diphosphate (20 mM). In the figure, the resonance of the uncomplexed FBA was arbitrarily set at 0 ppm.

The ^{19}F spectra of an FBA–D-glucose mixture as a function of pH are shown in Figure 7. In addition to a small resonance (peak II) at 7.55 ppm (relative to the free peak at pH 7.2), which can be observed at neutral pH, two additional resonances with shifts of 6.66 and 7.69 ppm (peaks I and III) grow at approximately the same rate as the pH is increased. The 7.69 ppm resonance also exhibits a shoulder which was resolvable in several of the

Table 2. Chemical Shifts of FBA Adducts[a]

compound	δ(FBA)[b]	δ(TFA)[c]
α-hydroxy carboxylates		
lactate	−6.46	−41.22
salicylate	−6.38	−41.14
catechols		
catechol	−6.68	−41.43
L-DOPA	−6.59	−41.34
pentoses		
ribose	−7.51	−42.27
ribose-5-P	−7.51	−42.26
ribulose	−7.49	−42.25
tetrose		
erythrose	−7.57	−42.32
triose		
glyceraldehyde-3-P	−7.40	−42.15
alditols		
mannitol	−6.57	−41.32
sorbitol	−6.51	−41.26
hexoses		
fructose	−6.88	−41.64
fructose-6-P	−7.62	−42.37
fructose-1-P	−6.93	−41.69
fructose-1,6-diP	−7.23	−41.99
glucose[d]	−7.55	−42.31
sorbose	−7.56	−42.31
NAD^+	−7.26	−42.01
2-pyridylcarbinol	−5.39	−40.14

[a] Shifts measured in 50 mM phosphate, pH 7.2, buffer, $T = 25$ °C. [b] Shifts relative to uncomplexed FBA. [c] Shifts relative to TFA. [d] Shift corresponds to the single glucose adduct resonance observed at pH 7.2.

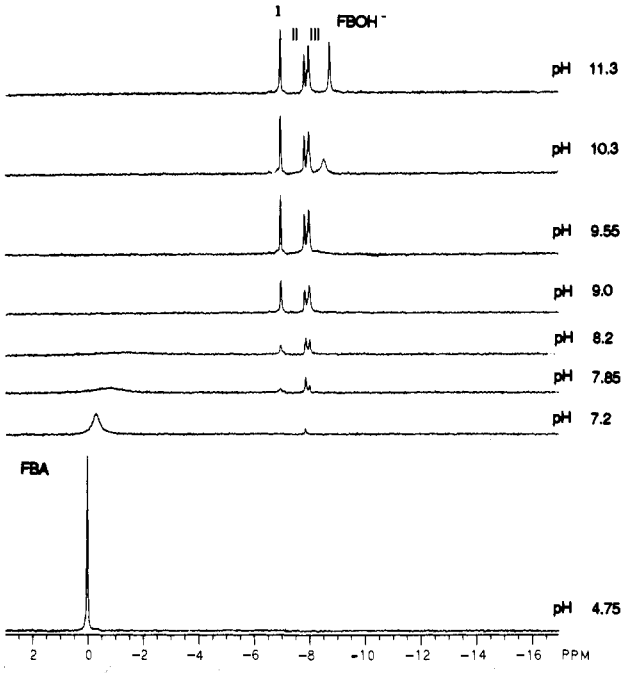

Figure 7. Proton-decoupled ^{19}F NMR spectra measured at 470.52 MHz of 3 mM FBA in the presence of 10 mM α-D-glucose. The buffer contained no phosphate, so that at intermediate pH values the resonance of uncomplexed FBA becomes broadened to the point of undetectability due to intermediate exchange between the acid and boronate species. In this figure, the ^{19}F shift of the 4-fluorobenzeneboronic acid at low pH was set equal to 0. However, we note that, in the discussion, the shifts are referenced relative to the FBA shift at pH 7.2, which is approximately 0.24 ppm upfield of the value for the acid form.

spectra, at ~7.6 ppm. Makkee et al.[10b] similarly observed three ^{11}B resonances for borate–glucose solutions at high pH and assigned these on the basis of the ^{11}B shift and additional ^{13}C data to a mixture of the α-D-glucofuranose 1,2:3,5-diborate and α-D-glucofuranose 1,2:5,6-diborate. These conclusions differ somewhat from an earlier proposal by de Bruyn and Anteunis[20] of a single 1,2:3,5,6-diborate species on the basis of ^1H NMR data. As discussed by Makkee et al.[10b] and by Chapelle and Verchere,[10g]

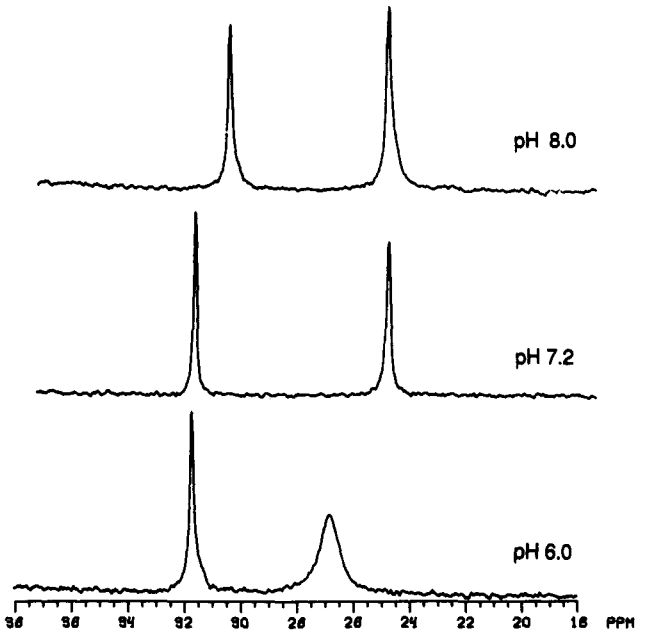

Figure 8. ^{19}F NMR spectra of FBA in the presence of sorbitol at the pH values indicated. Sample also contained 50 mM phosphate. Since the apparent dissociation constant increases significantly as the pH is lowered, the sorbitol concentration must be increased in order to observe the resonance of the complex. Sorbitol concentration was 8 mM at pH 8 and 80 mM at pH 6.

the binding of borate to the cis hydroxyl groups of the aldohexofuranoses is often sufficiently preferred to shift the equilibrium from pyranose to furanose forms. The three ^{19}F resonances observed for the FBA adduct at high pH may similarly correspond to adducts formed from the 1,2- the 5,6- and 3,5-hydroxyl groups of α-D-glucofuranose. Since the shift of peak I is similar to that observed for adducts with noncyclic alditols such as sorbitol, this resonance most probably corresponds to the 5,6-hydroxyl adduct. Alternatively, the shift of peak II is similar to that formed from furanoses such as ribose and would therefore most probably correspond to the 1,2-hydroxyl adduct. Peak III may therefore correspond to the 3,5-FBA adduct. However, as noted above, the possibility of *R* and *S* configurations for the 1,2-FBA adduct could also lead to the observed II and III resonances, as could a shift heterogeneity due to the presence of both 1,2-FBA and 1,2:5,6-diFBA adducts. A more complete assignment of the high-pH spectra would require additional ^{13}C and ^1H NMR studies, while the present effort was focused on the dynamic characterization of these adducts.

For ligands such as sorbitol which interact with FBA more strongly than glucose, it is possible to observe the ^{19}F resonance of the adduct at lower pH values if sufficient sorbitol is added. As the pH was lowered, the adduct resonance was observed to broaden and shift downfield, toward the resonance of the boronic acid (Figures 8 and 9). Considering a two-state system at equilibrium, the exchange between boronic acid and boronate adduct species can lead to exchange broadening, with the ratio of the exchange contributions to the line width related to the fractional concentrations according to

$$p_A \Delta\nu^A = p_B \Delta\nu^B \qquad (18)$$

where p_A (p_B) is the concentrations of boronic acid (boronate adduct) and $\Delta\nu^A = 1/\pi\tau_A$ ($\Delta\nu^B = 1/\pi\tau_B$) the exchange contribution to the line width of the acid (boronate adduct) in the slow exchange limit. However, examination of the spectra for FBA–sorbitol as a function of pH (Figure 8) indicates that exchange between the boronic acid and adduct species is not consistent with eq 18. Instead, the adduct is involved in another exchange process which is sufficiently rapid so that no additional ^{19}F resonance is observed but sufficiently slow to lead to a

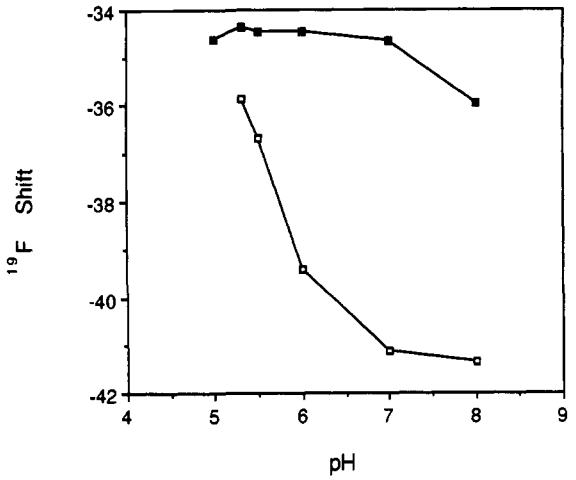

Figure 9. ^{19}F shift of FBA (○) and the FBA–sorbitol adduct (■) as a function of pH. At low pH, the ^{19}F shift of the adduct approaches that of fluorobenzeneboronic acid.

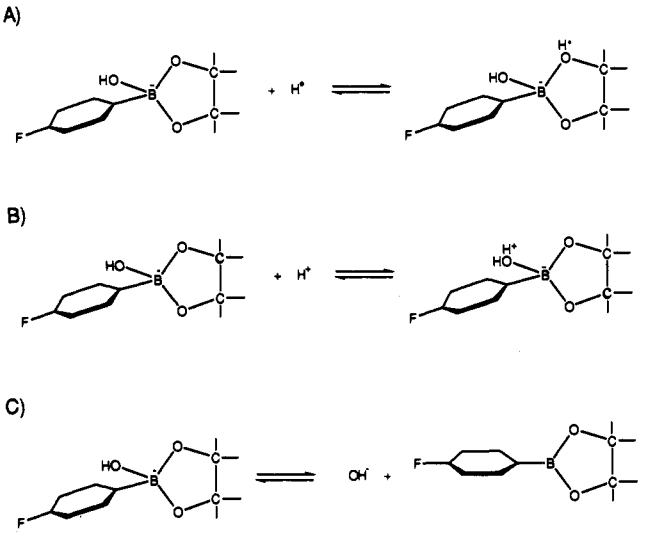

Figure 10. Possible equilibria with the FBA–sorbitol adduct: (A) protonation of oxygen ligand on sorbitol; (B) protonation of hydroxyl ligand; (C) reversible dehydroxylation.

significant broadening of the adduct ^{19}F resonance. Such processes could include reversible protonation of the adduct, as shown in Figure 10A, B, or reversible loss of the hydroxyl group to give a trigonal, boronic acid ester in which the sorbitol oxygens constitute both of the boronic acid oxygen ligands (Figure 10C). This type of complex has been known to form in organic solvents[22] and has recently been demonstrated in some cases in aqueous solutions as well.[10e,j] Fluorine-19 NMR spectra recorded as a function of pH indicate that as the pH is decreased, the chemical shift of the adduct becomes similar to that of the boronic acid species (Figure 9). This strongly suggests that the observed broadening corresponds to the equilibrium shown in Figure 10C, presumably involving an initial protonation as in Figure 10B. In addition, proton-exchange rates are often fast enough to result in shifts with minimal associated broadening, so that the large line width of the FBA–sorbital complex (Figure 8) would also be more consistent with hydroxide ion exchange.

Ligand-Exchange Kinetics of FBA Complexes

The kinetic behavior of FBA–ligand complexes was studied using magnetization transfer methods. Since at lower pH only two fluorine resonances were generally observed, the selective inversion technique of Robinson et al.[16] was applicable and, as

(22) Kinder, D. H.; Katzenellenbogen, J. A. *J. Med. Chem.* **1985**, *28*, 1917–1925.

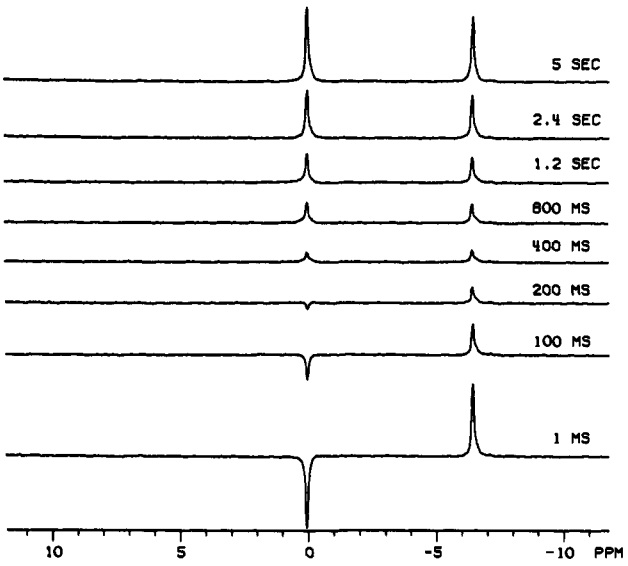

Figure 11. Half of a typical selective inversion experiment for a sample containing 20 mM FBA, 10 mM L-DOPA, 50 mM phosphate (pH 7.4), measured at 21 °C. The ^{19}F resonance of uncomplexed FBA was selectively inverted, and the magnetization transfer to the adduct is readily observed to be maximal at a delay near 400 ms. Typically a second experiment inverting the resonance of the adduct was carried out, and the resulting data were analyzed as described in Materials and Methods.

Table 3. Dissocation Rate Constants

	k_{-1}[a] (s^{-1})		literature values	
ligand	solv 1	solv 2	k_{-1} (s^{-1})	ligand
L-DOPA	8.5	4.5 4.0[d]		
4-methylcatechol		5.2	$4.0 \times 10^6[H^+]$	4-methylcatechol[b]
NAD^+	31	7.0		
lactate	120	84 56[d]	83	lactate[c]
			$3.8 \times 10^4[H^+]$	lactic acid[b]
sorbitol (pH 6.0)	42	6.1	$\sim 10^7[H^+]$	mannitol[b]
sorbitol (pH 7.2)	15	0.54 0.48[d] 3.6[e]		
sorbitol (pH 8.0)	3.8			

[a] Determined at 25 °C in 50 mM Sodium phosphate, pH 7.2, (solvent 1) or in 0.1 M KCl (solvent 2), [FBA] = 9 mM, and sufficient ligand to yield similar resonance intensities for the FBA and the adduct. [b] Ref 4. [c] Ref 2. [d] Conditions as above except that [FBA] = 2 mM. [e] Conditions as above except that [FBA] = 50 mM.

described in Materials and Methods, data were analyzed by carrying out sets of experiments in which the resonance of either the free FBA or the FBA–ligand complex was selectively inverted. This method proved generally ideal for such studies, since the kinetics are sufficiently slow to allow for the observation of separate resonances corresponding to free and bound species but are generally considerably faster than the fluorine T_1 (3.95 s for FBA at 25 °C) so that magnetization transfer effects are readily observed. In general, the use of short delay times in the Perrin and Engler formalism provides accurate values for the forward and reverse exchange rate constants but poorer accuracy for the spin–lattice relaxation rates for the present systems, since $k_{-1} \gg 1/T_1$. A typical magnetization transfer experiment for the L-DOPA adduct is shown in Figure 11. Dissociation rate constants for several ligands are summarized in Table 3.

It is immediately apparent that, analogous to the catalytic effects of phosphate buffer on the rate of hydroxyl ion exchange evident from Figure 2, the presence of buffers similarly accelerates the FBA–ligand exchange rate. A comparison of the dissociation rate constants observed in 50 mM phosphate and in 0.1 M KCl, used to maintain a similar ionic strength (Table 3), indicates that in all cases the rate is slower in the KCl, although the magnitude of the effect of the phosphate buffer is rather variable. The rates

obtained for FBA–sorbitol at pH 6.0 and 7.2 in 0.1 M KCl give the enhancement close to that expected for a proton-requiring dissociation process and are in reasonable quantitative agreement with a pseudo-first-order rate constant of $10^7[H^+]$ obtained by Pizer and Babcock[4] for the dissociation of mannitol–benzeneboronic acid. The dissociation rate constant for FBA–lactate measured in 0.1 M KCl is in close agreement with the value for dissociation of the lactate anion obtained by stopped-flow methods.[5] The pseudo-first-order dissociation rate constant of $3.8 \times 10^4[H^+]$ for the lactic acid–benzeneboronic acid complex given by Babcock and Pizer[5] indicates that this reaction would not be competitive with the non-proton-dependent anion dissociation process at neutral pH.

Alternatively, the dissociation rate constant for the L-DOPA complex was considerably faster than the value of $4.0 \times 10^6[H^+]$ obtained by Pizer and Babcock.[4] One complication of these studies is that, in the presence of catechols, a pH-dependent degradation of the FBA is observed, yielding 4-fluorophenol. Final concentrations of this degradative product based on ^{19}F resonance intensity ranged from 2.3% to 7.5% of the total FBA intensity for the systems studied. Problems with oxidation of the catechols at higher pH have been noted previously in stopped-flow kinetic measurements and significantly perturbed the measurements at pH 6.[4] However, we found that at pH 7.2 this process was quite slow and the separate 4-fluorophenol resonance observed did not interfere with the magnetization transfer studies. Since the quantity formed was small, and since the pK of 4-fluorophenol is sufficiently high that a buffering effect is not predicted, the effects of this degradative process on the measured rates were presumed negligible. A pair of matched samples of FBA + L-DOPA with and without 5 mM 4-fluorophenol gave identical rate constants, confirming this conclusion. Given the possibility of exchange catalysis by the amino group of L-DOPA, a study of the complex formed by FBA and 4-methylcatechol was also carried out and gave results which were in close agreement with the L-DOPA study (Table 3). Since the studies of Pizer and Babcock were carried out at pH 4, different dissociative processes may become operative at the higher pH of the NMR experiments.

In view of the significance of the intermolecular associative equilibria described, for example, by eq 17, several studies were carried out using higher or lower FBA concentrations. Increasing the FBA concentration from 9 to 50 mM significantly increased the dissociation rate constant for the sorbitol–FBA complex, indicating that an associative mechanism can become significant. Alternatively, reducing the FBA concentration from 9 to 2 mM resulted in relatively small changes in the rate for complexes with lactate, sorbitol, and L-DOPA. Thus, these preliminary data suggest that the associative mechanism becomes significant at high (tens of millimolar) concentration but may not be too significant below 10 mM.

It became particularly apparent in studies with imidazole ligands that some molecules could function both as ligands and as exchange catalysts. In the latter case, the ligand acts analogously to the buffer, transferring a proton to a hydroxyl or to a ligand oxygen leaving group of the adduct or, conversely, accepting a proton from water or from the ligand as it binds to the boronic acid. Since the ligand concentrations were adjusted in order to yield ~50:50 mixtures of FBA/FB–L, the ligand concentrations were also reduced along with the FBA concentrations. For ligands such as lactate which can act analogously to the buffers, changes in ligand concentration rather than in boronic acid concentration could explain any observed differences in rate constant. However, this is not the case for sorbitol, so that the results with this ligand are presumably due to associative equilibria, as described by eq 17.

Conclusions

The ^{19}F nucleus of 4-fluoro-substituted benzeneboronic acids provides a useful NMR probe for studying the interactions of the boron with various ligands. In addition to its high intrinsic sensitivity for NMR detection, the large chemical shift range results in slow chemical exchange characteristics for the adducts formed with many bidentate ligands, as well as for hydroxyl ion exchange at sufficiently low FBA concentration. Although equilibria involving boronates are simpler than those involving borate due to the more limited binding stoichiometry of the adducts formed, the kinetic behavior is complex. Analysis of line-width data for the hydroxyl exchange reaction indicates that, at typical concentrations used for NMR studies, intermolecular associative interactions involving the transfer of a hydroxyl group from boronate to boronic acid dominate the observed kinetic behavior. The initially unexpected result of faster kinetics for CFBA compared with FBA, in contrast to the results of stopped-flow kinetic measurements for the analogous nonfluorinated compounds,[3] is seen to be a consequence of the greater rate constant for the intermolecular transfer in the former (Table 1). The greater rate constant for CFBA could reflect a greater tendency of the more hydrophobic CFBA to ring stack. For example, chlorobenzene exhibits a larger octanol/water partition coefficient than benzene[23] and exhibits larger retention factors in a variety of reversed-phase chromatography systems.[24] In agreement with earlier conclusions based on stopped flow measurements,[3] it is concluded that mechanisms involving initial protonation of the boronate species and subsequent loss of H_2O are not significant near the neutral pH range at which the compounds of the present study were observed. However, a variety of buffers were found to significantly catalyze dissociation of the boronate hydroxyl group, presumably due to a proton-transfer step. Such a transfer could occur prior to, concerted with, or subsequent to the loss of the hydroxyl group, with the latter process reducing the probability of reassociation.

Rate constants $k_{-4} = 2.5 \times 10^8$ and 2×10^7 M^{-1} s^{-1} for the interaction of boronate with imidazole and phosphate were obtained. The rate obtained with imidazole appears to be approaching a diffusion-controlled limit.[25] These rates are consistent with the maximum value of the proton-catalyzed dissociation rate of 1.6×10^{10} M^{-1} s^{-1}, obtained in the absence of buffers. At neutral pH, this corresponds to a maximum rate of 1600 s^{-1}, which is much less than the rate due to intermolecular boronic acid–boronate hydroxyl ion transfer at the concentrations studied. The rate acceleration due to the positively charged imidazolium ion would probably be most similar to k_{-2} corresponding to the interaction of H_3O^+ with the boronates.

Inversion transfer studies of the kinetic behavior of slowly exchanging bidentate boronate adducts indicate that the same mechanisms responsible for hydroxyl ion dissociation are operative. Dissociation rates for all ligands tested were significantly accelerated by 50 mM phosphate, and there is a significant rate enhancement at higher (50 mM) FBA concentrations. Alternatively, declines in the rate constants at 2 mM FBA were relatively modest, and it is possible that the contribution of associative equilibria between FBA and the boronate adducts is less significant than in the case of hydroxyl ion transfer.

(23) (a) Hansch, C.; Leo, A. J. *Medchem Project Issue No. 26*; Pomona Collage: Claremont, CA, 1985. (b) Hansch, C.; Leo, A. J. *Substituent constants for correlation analysis in chemistry and biology*; John Wiley & Sons: New York, 1979; p 197.

(24) Melander, W. R.; Horvath, C. In *Reversed-phase chromatography, in High-performance liquid chromatography*; Horvath, C., Ed.; Academic Press: New York, 1980; Vol. 2, pp 182–185.

(25) Davis, M. E.; Madura, J. D.; Sines, J.; Luty, B. A.; Allison, S. A.; McCammon, J. A. *Methods Enzymol.* **1991**, *202*, 473–497.